Theory of the quadrupolar deformability in silver halides

W. G. Kleppmann and W. Weber*

Max-Planck-Institut für Festköperforschung, Heisenbergstrasse 1, 7 Stuttgart-80, West Germany

(Received 28 December 1978)

The tight-binding method of Varma and Weber is used to calculate phonon dispersion curves in silver halides. For this purpose the method is extended to include crystal-field matrix elements in the electron-phonon coupling. It is shown that the quadrupolar deformability of Ag^+ ions, as proposed in the model of Fischer et al., arises indeed from virtual atomic Ag^+ d-s excitations induced by displacements of the neighboring halide-ion potentials. In the limit of flat bands there is an exact correspondence of model and microscopic quadrupolar terms. Moreover, realistic band-structure calculations do not significantly alter the above results. We use self-consistent ionic wave functions to obtain numerical estimates for the absolute magnitude of the quadrupolar deformability in fcc AgCl, AgBr, and AgI. With these numbers we get good agreement with the phonon dispersion curves, using an otherwise simple shell model. For AgI we predict with reasonable short-range parameters that the crystal is unstable, thus suggesting a reason for the different structure of AgI at atmospheric pressure.

I. INTRODUCTION

It has been known for some time that the phonon dispersion curves of cubic silver halides show some unusual features, most notably a lowering of the energies of some optic phonons (as compared to alkali halides). This effect is particularly dramatic at the L point of the Brillouin zone, where the TO phonon has a very low energy. Fischer et al.[1] and Fischer[2] have been able to fit this feature with a shell model into which they introduced additionally a quadrupolar deformability at the Ag^+ ion. They argued that this deformability is important in the cubic silver halides due to virtual d-s excitations at the Ag^+ ions. These should be made possible by the relatively small band gap between occupied valence bands—having appreciable Ag-d character—and the lowest empty conduction band of predominatly Ag-s character.

The model has been quite successful. It has predicted the exchange of wave vectors between the TO and TA phonons at the L point in AgBr, which has been verified experimentally,[3] and it has led to a good overall fit of the phonon dispersion curves in AgCl[1,2] and AgBr.[3] The idea of the quadrupolar deformability as an intrinsic property of the coupling of the silver ion to its neighbors has also been applied to get an explanation of the low-activation energy for silver motion in AgCl and AgBr,[4] and the unusual symmetry of Ag^+ defects in RbCl and RbBr.[5]

First-principles investigations of this problem have not been carried out so far. The closest to it comes from a paper by Zeyher.[6] He has presented a microscopic theory of the lattice dynamics of alkali halides and shown that in the limit of flat bands, i.e., a large electronic band gap compared to the bandwidth, his expressions for the contribution of the longitudinal degrees of freedom could be arranged to yield dipolar, breathing-like, and quadrupolar deformations of the electronic charge. However, for alkali halides the quadrupolar deformability turned out to be negligibly small compared to the others.

In this paper we give an ab initio derivation of the quadrupolar deformability of Ag^+ in the cubic Ag halides starting from a more general approach which allows us to include the dispersion of the electronic bands, namely, the formalism of Varma and Weber (VW).[7] The latter uses a nonorthogonal tight-binding (NTB) representation of the band structure and gives expressions for the change of the one-electron energies due to the ionic displacements by a phonon in terms of derivatives of the energy transfer and overlap matrix elements.

In Sec. II, this treatment is briefly reviewed and generalized to include crystal-field terms. In Sec. III we show analytically how s-d crystal-field matrix elements (i.e., matrix elements between s and d wave functions on the silver ion with the potential of the neighboring halogen ions) reduce, in the limit of flat bands, to the quadrupole term with E_g symmetry (from the longitudinal coupling, as in Ref. 6) and a new term with T_{2g} symmetry from the transverse part. A simple expression for the prefactor is obtained. In Sec. IV we compare the numerical results from the full expression of Sec. II with the analytical formulas. Finally in Sec. V we apply our results to the lattice dynamics of fcc silver halides and discuss their implications for the high ionic conductivity of these materials. The conclusions are summarized in Sec. VI.

II. OUTLINE OF OUR APPROACH

As has been mentioned in the introduction we are going to follow the formalism of Varma and Weber.[7] This theory has been developed for applications in transition metals[7-9] and their compounds[10] (TMC). In these studies it becomes evident that all the sharp features in the dispersion curves of these materials are obtained by considering only the change of the total one-electron energy of the crystal with ionic displacements. The electronic band structure is described in a nonorthogonal tight-binding scheme as a natural formalism for transition metals.

Compared to the conventional theory of lattice dynamics,[11] the approach of Varma and Weber employs a different grouping of the various contributions to the dynamical matrix. The first term is the change of the sum of all one-electron energies up to second order in displacements, the other (D_0 in the VW notation) is the difference of the direct ion-ion and electron-electron interaction (the latter being double counted in the one-electron energies). The first contribution is again divided in two parts. D_1 arises from changes of the one-electron energies to first order in perturbation theory. The other term D_2 is second order in perturbation theory and involves tight-binding matrix elements linear in the ionic displacements. In elemental crystals, e.g., transition metals like Nb, Mo, it can be shown that D_0 and D_1 lead essentially only to short-range force constants whereas D_2 is found to be the source of all sharp structure in the phonon dispersion curves of these materials. In compounds where charge transfer from one to the other atom occurs, D_0 and D_1 may also give rise to long-range forces of Coulombic type. But again, in the case of transition-metal carbides and nitrides, the sharp structure in the acoustic phonons arises from D_2.

Although it is possible in principle to calculate all terms in the VW formalism, the interest has focused on calculating D_2; D_0 and D_1 have been fitted by short-range force constants. In this paper we will follow this line and will investigate only D_2 microscopically. In an obvious generalization of the expression of VW this is given by

$$D_2(\lambda\alpha, \lambda'\beta|q) = -\sum_{\substack{k,\mu,\mu' \\ k'=k+q}} \frac{f_{k'\mu'} - f_{k\mu}}{E_{k\mu} - E_{k'\mu'}}$$

$$\times g^{\lambda\alpha}_{k\mu,k'\mu'} g^{\lambda'\beta}_{k'\mu',k\mu} \quad . \qquad (1)$$

Here $E_{k\mu}$ is the energy of an electron with wave vector k in the band μ and $f_{k\mu}$ is the occupation number for this state. $g^{\lambda\alpha}_{k\mu,k'\mu'}$ is the electron-phonon matrix element, giving the coupling between the electronic states $k\mu$ and $k'\mu'$ induced by a displacement of the ion λ in the direction α. q is the wave vector of the

phonon. The sum goes over all scattering processes from occupied electronic states to unoccupied states. The virtual d-s excitations which were invoked by Fischer et al.[1] are contained as a special case in Eq. (1), as will be shown later. But Eq. (1) allows us to study the electronic contributions to the dynamical matrix in a more general way, in particular, we can see what further approximations have to be made to obtain the quadrupolar deformability and how good these approximations are. This will be done in detail in Secs. III–VI. Here we are going to derive expressions for the electron-phonon coupling matrix g. This requires some modifications and generalizations compared to TMC.

(i) We now deal with a diatomic compound which is clearly ionic in character; i.e., the charge transfer from the silver to the halide leads to long-range Coulomb forces, modifying all contributions to the dynamical matrix. The parts not explicitly included in D_2 are described within a normal-shell model.

(ii) Unlike the situation in TMC, where the important contributions to D_2 come from excitations within the d bands close to the Fermi surface, in silver halides the contributions arise from scattering from the valence to the conduction band.

(iii) Due to the Coulomb potentials of all the ions "crystal-field terms" (coupling between wave functions on the same ion, induced by the potential of the neighbors) become important.

We now sketch the necessary additions and refer to the Refs. 8–10 for an extensive derivation of the formalism.

D_2 as given in Eq. (1) requires the knowledge of the equilibrium one-electron energies which are found as solutions of the nonorthogonal tight-binding (NTB) Hamiltonian

$$H'U = S^{-1/2}HS^{-1/2}U = EU \quad , \qquad (2)$$

where E is the diagonal matrix of eigenvalues $E_{k\mu}$. U is the appropriate unitary transformation for diagonalizing the NTB Hamiltonian H'. The matrix

$$H(\kappa m, \kappa'm'|k) = N^{-1} \sum_{l,l'} H(l\kappa m, l'\kappa'm')$$

$$\times \exp(ikR(l\kappa, l'\kappa')) \qquad (3)$$

is the Fourier transform of the real-space tight-binding (hopping) matrix elements

$$H(l\kappa m, l'\kappa'm') = \int \phi^*(l\kappa m) H \phi(l'\kappa'm') d^3r \qquad (4)$$

of the Hamiltonian H between the ionic wave function of type m centered on the ion κ in unit cell l and the wave function m' on ion κ' in cell l'. S is the corresponding matrix with H replaced by 1 (overlap matrix). These matrix elements are listed, e.g., by Slater and Koster.[12] $R(l\kappa, l'\kappa')$ is the distance vector

between the sites $(l\kappa)$ and $(l'\kappa')$. For the electron-phonon matrix g we need the derivatives of the Hamiltonian matrix H and the overlap matrix S. We use a two-center approximation. Then we have to distinguish two cases in Eq. (4).

(a) The sites of the wave functions $(l\kappa) \neq (l'\kappa')$.

The potential part of the Hamiltonian must then be located on $(l\kappa)$ or $(l'\kappa')$. These are the normal "hopping" matrix elements, which enter into the dispersion of the electronic bands. For more than one particle per unit cell, their contribution to the electron-phonon matrix reads[10]

$$g^{\lambda\alpha}_{k\mu,k'\mu'} = \sum_{\substack{\kappa,m \\ \kappa',m'}} A^*(\kappa m \,|\, k\mu)\, [\gamma_\alpha(\kappa m, \kappa'm' \,|\, k')\delta_{\kappa\lambda} - \gamma_\alpha(\kappa m, \kappa'm') \,|\, k)\delta_{\kappa'\lambda}] A\,(\kappa'm' \,|\, k'\mu') \quad . \tag{5}$$

A is related to U by

$$A = S^{-1/2} U \tag{6}$$

and the matrix γ is defined as

$$\gamma_\alpha(\kappa m, \kappa'm' \,|\, k) = N^{-1} \sum_{l,l'} [\nabla_\alpha H(l\kappa m, l'\kappa'm') - \epsilon \nabla_\alpha S(l\kappa m, l'\kappa'm')]\, \exp(ikR\,(l\kappa, l'\kappa')) \tag{7}$$

with $\epsilon = \frac{1}{2}(E_{k\mu} + E_{k'\mu'})$. $\nabla_\alpha H$ and $\nabla_\alpha S$ are the real-space derivatives of the tight-binding matrix elements.

(b) "Crystal-field" matrix elements have both orbitals at the same atom $[(l\kappa) = (l'\kappa')]$, but the potential is due to a neighboring site. In band-structure calculations these terms are not immediately evident, as they do not give any dispersion to the bands. In many cases they cancel when summed over a shell of neighbors. They only show up in the splitting of atomic energies in the crystal field, which, in the case of cubic symmetry, only affects orbitals with quantum number $l \geq 2$, but not s or p orbitals.

Let us denote a crystal-field matrix element by

$$C(l\kappa m, l\kappa m'; l'\kappa') = \int \phi^*(l\kappa m)\, V(l'\kappa')\, \phi(l\kappa m')\, d^3r \quad , \tag{8}$$

where $V(l'\kappa')$ is the potential of the ion $(l'\kappa')$. We then define

$$C_\alpha(\kappa m, \kappa m', \kappa'|q) = N^{-1} \sum_{l,l'} \nabla_\alpha C\,(l\kappa m, l\kappa m'; l'\kappa')$$
$$\times \exp(iqR\,(l\kappa, l'\kappa')) \quad . \tag{9}$$

Note that this is independent of the electronic wave vector k, since the two electronic wave functions are on the same site $(l\kappa)$ (for the same reason they do not contribute to the electronic dispersion). In the contributions to g, we have to distinguish the cases:

(i) $\kappa = \kappa'$, i.e., wave function and potential are at the same sublattice atoms (but of course not at the same site). Here we get

$$g^{\kappa\alpha}_{k\mu,k'\mu'} = \sum_{m,m'} A^*(\kappa m \,|\, k\mu)\, [C_\alpha(\kappa m, \kappa m', \kappa|0)$$
$$- C_\alpha(\kappa m, \kappa m', \kappa|q)]\, A\,(\kappa m' \,|\, k'\mu') \quad . \tag{10}$$

The contribution from the other sublattices vanishes.

(ii) $\kappa \neq \kappa'$. For the case that the wave function is at the sublattice κ atoms and the potential on κ', we get

$$g^{\kappa\alpha}_{k\mu,k'\mu'} = \sum_{m,m'} A^*(\kappa m \,|\, k\mu)$$
$$\times C_\alpha(\kappa m, \kappa m', \kappa'|0)\, A\,(\kappa m' \,|\, k'\mu') \quad , \tag{11}$$

$$g^{\kappa'\alpha}_{k\mu,k'\mu'} = -\sum_{m,m'} A^*(\kappa m \,|\, k\mu)$$
$$\times C_\alpha(\kappa m, \kappa m', \kappa'|q)\, A\,(\kappa m' \,|\, k'\mu') \quad .$$

The contributions from different crystal-field terms are additive in g, which means that there can be interference terms in D_2.

III. ANALYTICAL TREATMENT FOR FLAT BANDS

In the limit of flat bands, all off-diagonal Hamiltonian and overlap matrix elements in Eq. (2) are ignored. Their derivatives are also neglected and we retain only nearest-neighbor crystal-field terms. Then the contributions to g from Eqs. (5) and (10) vanish and the only nonvanishing terms arise from Eq. (11). If we now assume that the band structure can be represented by filled Cl-p and Ag-d valence bands and an empty Ag-s conduction band, then the only crystal-field matrix elements connecting a filled with an empty band are matrix elements between Ag-d and Ag-s wave functions $(\kappa = 1)$ with the potential of the neighboring Cl$^-$ ion $(\kappa' = 2)$. Equation (11) then becomes

$$g^{1\alpha}_{k\mu,k'\mu'} = \sum_{m,m'} A^*(1m \,|\, k\mu)\, C_\alpha(1m, 1m', 2|0)$$
$$\times A\,(1m' \,|\, k'\mu') = 0 \quad , \tag{12}$$

$$g^{2\alpha}_{k\mu,k'\mu'} = -\sum_{m,m'} A^*(1m \,|\, k\mu)\, C_\alpha(1m, 1m', 2|q)$$
$$\times A\,(1m' \,|\, k'\mu') \quad , \tag{13}$$

where m and m' denote the s or a d orbital on the

silver ion, respectively. In Eq. (12) we have used the fact that a matrix element between s and d wave functions is even; its derivative, therefore, is odd. Then we see immediately from Eq. (1) that the new contribution to the dynamical matrix is nonvanishing only in the Cl-Cl submatrix.

$$\Delta D(\text{Cl}-\text{Cl}) = -\frac{4(sd\sigma')^2}{E_S - E_E}\begin{vmatrix} 2\sin^2 x & -\sin x \sin y & -\sin x \sin z \\ -\sin x \sin y & 2\sin^2 y & -\sin y \sin z \\ -\sin x \sin z & -\sin y \sin z & 2\sin^2 z \end{vmatrix} - \frac{24(sd\sigma)^2}{a^2(E_S - E_T)}\begin{vmatrix} \sin^2 y + \sin^2 z & \sin x \sin y & \sin x \sin z \\ \sin x \sin y & \sin^2 x + \sin^2 z & \sin y \sin z \\ \sin x \sin z & \sin y \sin z & \sin^2 x + \sin^2 y \end{vmatrix}.$$

(14)

Here, $x = q_x a$, $y = q_y a$, $z = q_z a$, $(sd\sigma)$ is the s-d crystal-field matrix element, and $(sd\sigma')$ is its radial derivative, a is the nearest-neighbor separation, E_s is the energy of the Ag-s band, E_E is the energy of the E_g part, and E_T is the energy of the T_{2g} part of the Ag-d band. The factors $\sin x$, etc., are a result of summing over the $\exp(iqR(l\kappa,l'\kappa'))$ because of the odd symmetry of the derivatives of the s-d matrix elements in Eq. (9).

The first part of Eq. (14) has exactly the form of the quadrupolar deformability considered by Fischer et al.[1,2] and Zeyher.[6] It arises from the longitudinal coupling to the nearest neighbors, as is manifest by the fact that it is related to the radial derivative of the matrix element. The second term has T_{2g} symmetry and arises from the transverse coupling—it involves the transverse derivatives of the matrix elements. This term has not been included in the treatment by Zeyher.[6] In the model of Fischer et al.[1,2] a term with T_{1g} symmetry has been considered instead, which differs only in the sign of the off-diagonal terms. However, we find no justification for it in this calculation.

IV. NUMERICAL CALCULATIONS

First of all we study the effect of a realistic band structure on our results. To do this we use a nonorthogonal tight-binding fit to the pseudopotential band structure of Wang et al.[13] for AgCl, based on s and d wave functions on the silver and p wave function on the chlorine ion allowing nearest-neighbor Ag-Cl, Ag-Ag, and Cl-Cl interactions. The overall fits were very good, differing by at most 0.01 Ry for the valence band and 0.08 Ry for the conduction band. For comparison we also used tight-binding band structures of Smith[14] for AgCl and AgI in our calculation.

Ignoring for the moment all derivatives of matrix elements except for the $sd\sigma$ crystal-field matrix elements we evaluate the k summations for the band

Using the fact that the potential has s-like symmetry, the angular dependence of the crystal-field matrix elements can be taken directly from Slater and Koster.[12] Their derivatives can be evaluated analytically. Substituting their form into Eq. (13) and summing over all d orbitals in (m,m') finally gives

structures mentioned using a program due to Diamond[15] for a large number of q points throughout the Brillouin zone. For all three band structures the results differ by less than 2% from the analytical form (14). The effective energy denominators are given in Table I. They are not very different for the E_g and T_{2g} case and the numbers of the two different band structures for AgCl agree to within 4%. Their magnitude corresponds to a medium separation between valence and conduction band, as of course it should be.

The small departure from the flat-band limit can be understood by bearing in mind that the matrix elements are independent of the electronic wave vector k and that it only enters via the energy denominator. Since we are dealing with an insulator however, the variation in the energy denominator between different k-values is about a factor 2 only (contrary to metals, where scattering near the Fermi surface dominates). And even this small variation tends to be averaged out by the summation over k vectors, where particularly small energy denominators also get a small weight, because generally they are small only over a fraction of the Brillouin zone.

Thus as far as the q dependence of the extra term in the dynamical matrix is concerned, the flat-band approximation gives very good results; the band-structure information is only necessary to get the correct value for the effective-energy denominator.

TABLE I. Effective energy denominators obtained from tight-binding band structure (Ry).

	$E_S - E_E$	$E_S - E_T$
AgCl (Wang et al.)	0.667	0.656
AgCl (Smith)	0.642	0.636
AgI (Smith)	0.617	0.643

Next we have to test whether the *sd* crystal-field matrix element really gives an important contribution to the dynamical matrix. To this end we use reasonable estimates for all the radial derivatives of matrix elements (the transverse parts are already determined by the matrix elements themselves, which in turn are given by the band structure). In this way we get the following results:

(a) *pp*, *dd*, *ss*, and *pd* matrix elements do not contribute much, since there is very little *p* and *d* admixture to the conduction band and *s* admixture to the valence band (maximally 15% and even that only over a small region of the Brillouin zone). So their contribution is suppressed by a factor well above 10. Furthermore *pp*, *dd*, and *ss* matrix elements are small anyway, since they connect next-nearest neighbors only.

(b) *sd* normal matrix elements are small (smaller by a factor of 40 than *pd* σ), since they connect next-nearest neighbors only. The overall contribution of (a) and (b) together was found to be about 10% of the crystal-field contribution.

(c) *sp* matrix elements are large and they contribute directly to the scattering, since, to a first approximation, *s* is empty and *p* is full. However, they have dipole symmetry. In our treatment above we have ignored both the short-range and the long-range Coulombic terms (which of course are important in ionic crystals, as has been shown by the success of the shell models and by direct expansion of the interaction between the ions). So to be consistent with the other approximations, we have included these dipole effects in the simple-shell model which should describe the "normal" lattice dynamics. Our aim in this paper is only to identify and calculate terms that go beyond this normal-shell model.

(d) Of course there are also interference terms between the different contributions, but these are typically 10% of the individual contributions.

V. APPLICATION TO THE LATTICE DYNAMICS

A. Magnitude of the matrix elements

In Sec. IV we found that Eq. (14) is a very good approximation to the electronic contribution to the lattice dynamics going beyond the simple-shell model. If we use the numbers given in Table I for the energy denominators, it only remains to calculate the *sd* σ crystal-field matrix element and its radial derivative.

For this calculation we use self-consistent ionic wave functions and potentials obtained in a local density approximation. For the exchange-correlation contribution to the potential we use two different approximations:

$$V_{xc} = -\tfrac{2}{3}\rho^{1/3} + \cdots \ , \tag{15a}$$

TABLE II. Crystal-field matrix elements and radial derivatives.

		sd σ (Ry)	$\dfrac{d \ln(sd\,\sigma)}{dr}$ (Bohr rad.$^{-1}$)
AgCl	(AH)	−0.019 72	−1.44
AgCl	(HS)	−0.016 72	−1.27
AgBr	(AH)	−0.022 28	−1.26
AgBr	(HS)	−0.019 48	−1.15
AgI	(AH)	−0.029 74	−1.16
AgI	(HS)	−0.030 80	−1.01

where the dots stand for the Wigner interpolation term,

$$V_{xc} = -\rho^{1/3} \ . \tag{15b}$$

Equation (15a) has been employed by Appelbaum and Hamann (AH) in their self-consistent linear combination of atomic orbitals (LCAO) band-structure program.[16] Equation (15b) is the Slater exchange potential and has been used by Herman and Skillman (HS).[17] We use both exchange potentials to evaluate the crystal-field matrix elements and their derivatives for AgCl, AgBr, and fcc AgI. The results are summarized in Table II. We now use the energy denominators from Table I with the band structure of Smith[14] (the results of Wang *et al.*[13] for AgCl differ only very little) for AgCl and AgI, and linearly interpolated values for AgBr, and evaluate the prefactors of the matrices in Eq. (14) which we denote by

$$s^{E_s} = \frac{4(sd\,\sigma')^2}{E_s - E_E} \ , \tag{16a}$$

$$s^{T_{2g}} = \frac{24(sd\,\sigma)^2}{a^2(E_s - E_T)} \ . \tag{16b}$$

The results are given in Table III. They show that

TABLE III. Prefactors s^{E_g} and $s^{T_{2g}}$ of the extra terms in the dynamical matrix in units of e^2/V.

		s^{E_g}	$s^{T_{2g}}$
AgCl	(AH)	1.43	0.16
AgCl	(HS)	0.80	0.11
AgBr	(AH)	1.58	0.20
AgBr	(HS)	1.01	0.16
AgI	(AH)	2.88	0.39
AgI	(HS)	2.36	0.42

TABLE IV. Shell-model parameters used in the calculations (in addition to s^{E_g} and $s^{T_{2g}}$).

		AgCl	AgBr	AgI(E_1)	AgI(E_2)
A_{+-}	(e^2/V)	12.60	13.07	13.60	13.60
B_{+-}	(e^2/V)	−1.90	−2.05	−2.20	−2.20
A_{--}	(e^2/V)	1.09	1.65	2.20	2.20
B_{--}	(e^2/V)	−0.19	−0.12	−0.05	−0.05
Y^+	(e)	2.00	2.33	2.33	2.53
Y^-	(e)	−6.14	−7.94	−7.94	−11.69
k^+	(e^2/V)	109	93	93	79
k^-	(e^2/V)	557	964	964	2163

the matrix elements obtained by using the AH wave functions are consistently larger than with the HS wave functions. The reason is that the AH potential leads to a somewhat too large extent of the halide-ion wave functions. We thus employ HS wave functions in the following. The discrepancy between the two results is a measure for their uncertainty.

In all cases the E_g deformability is considerably larger than the T_{2g} part. This can be understood qualitatively, by noting that for a Coulomb potential the lowest-order contribution to the sd matrix element is r^{-3}, i.e., that the radial derivative is three times the transverse derivative. Thus we expect that $s^{E_g} = \frac{3}{2} s^{T_{2g}}$. For the true potential, the r dependence is going to be more rapid, hence increasing the radial

derivative even more and thus increasing s^{E_g}. A separation dependence of the matrix element $sd\sigma$ between r^{-6} and r^{-8} accounts approximately for the calculated difference; this is quite reasonable.

B. Lattice dynamics

We now use the values for s^{E_g} and $s^{T_{2g}}$ which we have calculated from the band structure with the HS ionic wave functions and fit the other parameters of a simple-shell model (8 parameters) to the dispersion curves of AgCl and AgBr. In both cases very good fits are obtained using the parameters listed in Table IV. In Figs. 1 and 2 the theoretical curves are com-
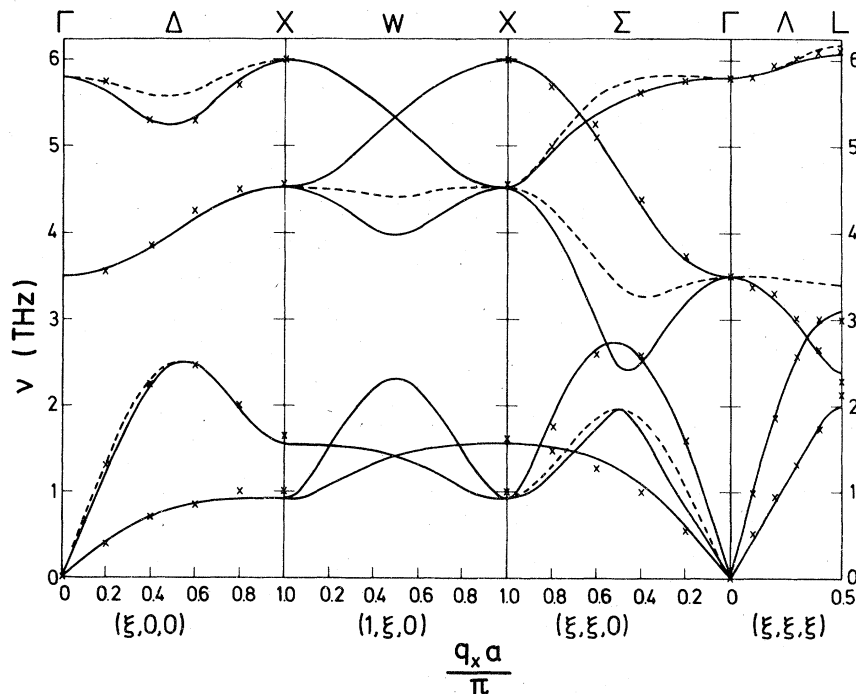

FIG. 1. Calculated phonon dispersion curves of AgCl (line) compared to experiment (crosses) [Vijayaraghavan et al. (Ref. 18)].
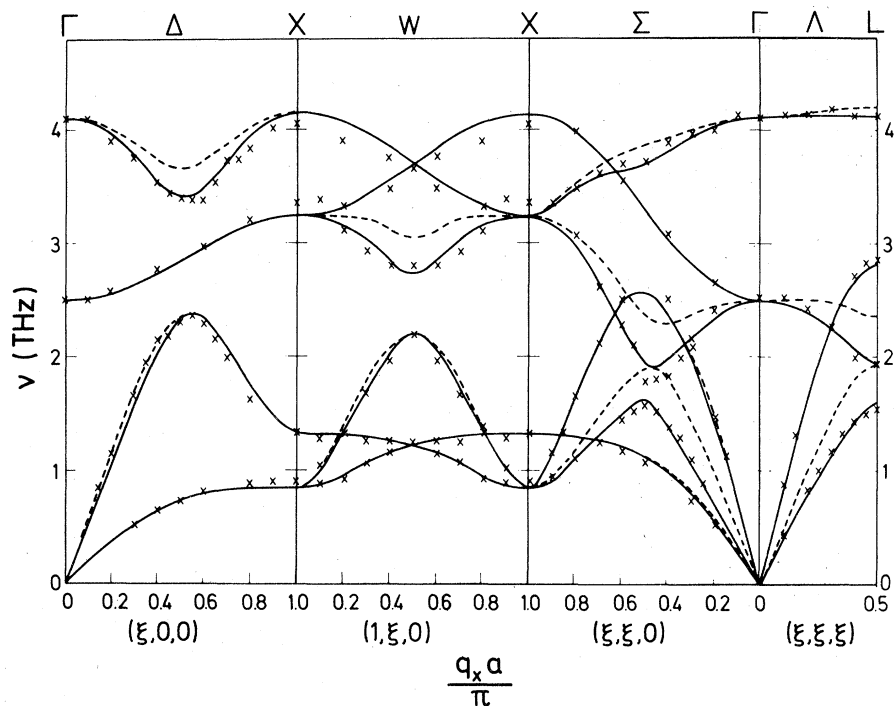
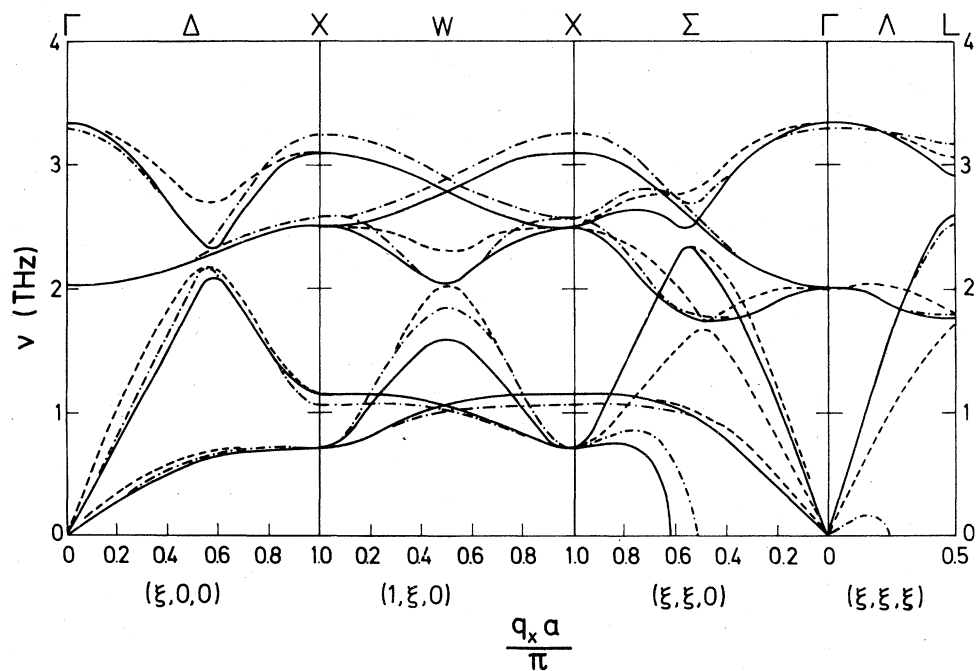FIG. 2. Calculated phonon dispersion curves of AgBr (line) compared to experiment (crosses) [Dorner *et al.* (Ref. 3)]

FIG. 3. Calculated phonon dispersion curves of fcc AgI ——— short-range parameters as for AgBr, with deformabilities, — — — — short-range parameters as for AgBr, without deformabilities, —·—·— short-range parameters extrapolated (E_2 in Table IV), with deformabilities.

pared with the experiment. The dashed lines show the dispersion curves with the same parameters but without the extra contributions to the dynamical matrix. They demonstrate that the main effects of the extra contributions are on the optic branches at wave vectors containing $\frac{1}{2}$, but that also some acoustic phonons are pushed to lower energies, in particular the TA branch in the (ξ, ξ, ξ) direction and the TA1 branch in the $(\xi, \xi, 0)$ direction (for a discussion of the elastic constants see below).

We now use various extrapolations to get an idea of the lattice dynamics of hypothetical fcc AgI. For AgI we always take $s^{E_g} = 2.36$ and $s^{T_{2g}} = 0.42$ as given in Table III. For the other parameters, we use three sets: (a) the same as AgBr; (b) the short-range parameters are linearly extrapolated [AgI(E_1) in Table IV]; (c) y/k and y^2/k are also linearly extrapolated [AgI(E_2) in Table IV]. The results for (a) and (c) are shown in Fig. 3; (b) is omitted for clarity, but it is very similar. The most surprising result is that in all three cases the TA1 phonon in the $(\xi, \xi, 0)$ direction is unstable about half way to the zone boundary and the TA phonon in the (ξ, ξ, ξ) direction is unstable for all k [case (a)] or for k values between about 0.2 and 0.5 [cases (b) and (c)]. Similar results are obtained for a wide range of shell model parameters. If the calculation is repeated for $s^{E_g} = 0 = s^{T_{2g}}$, the lattice dynamics is perfectly normal in all cases [case (a) is shown in Fig. 3 (dashed)]. This comparison suggests that the quadrupolar deformability may be responsible for the instability of fcc AgI at normal pressure, as is observed experimentally. At high pressures the short range repulsion parameters increase which can serve to stabilize the lattice again.

s^{E_g} and $s^{T_{2g}}$ also have a very marked effect on the elastic constants. In Table V we compare the elastic constants of AgCl, AgBr, and the hypothetical fcc AgI with and without the extra terms s. The table shows clearly a decrease of c_{11} and c_{44}, and a very marked increase of c_{12}, when s is introduced. Whereas $c_{12}/c_{44} \approx 3$ for $s = 0$, it increases to ≈ 5 for the s calculated microscopically. Thus it gives an important contribution to the violation of the Cauchy relation in the silver halides, as has previously been noted by Fischer et al.[2] However, even more marked is the decrease of $c_{11} - c_{12}$ due to the presence of the extra terms. In fcc AgI, $c_{11} - c_{12}$ even becomes negative (this accounts for its instability).

Since a simple continuum theory of the activation

TABLE V. Elastic constants (10^{11} dyne/cm^2) with and without s^{E_g} and $s^{T_{2g}}$.

		c_{11}	c_{12}	c_{44}
AgCl	(with s)	6.79	3.94	0.81
AgCl	($s = 0$)	8.38	3.13	0.92
AgBr	(with s)	6.38	3.76	0.84
AgBr	($s = 0$)	8.09	2.89	0.98
AgI	(a, with s)	3.25	3.93	0.50
AgI	(b,c, with s)	4.03	4.10	0.65
AgI	($a, s = 0$)	6.47	2.32	0.78

energy for hopping of ions in AgCl and AgBr (Ref. 4) shows that the activation energy is proportional to $(c_{11} - c_{12} + 3c_{44})$ it is clear that the extra contributions to the lattice dynamics lead to a drastic decrease of the activation energy. This combined with the instability of fcc AgI suggests again a reason for the high ionic conductivity of AgI and other silver compounds.

VI. CONCLUSIONS

We have used the method of Varma and Weber as a simple technique to single out terms in the dynamical matrix for the phonons of silver halides, which correspond to quadrupolar deformabilities of the Ag$^+$ ion. We have estimated the magnitudes of the E_g and T_{2g} deformabilities and then used these values to obtain otherwise simple-shell model fits to the dispersion curves of AgCl and AgBr. Extrapolation to AgI suggests that the E_g and T_{2g} deformabilities are responsible both for the instability of the fcc structure at normal pressures and the low-activation energies for ionic hopping and hence for the high-ionic conductivity.

*Present address: Kernforschungszentrum, Karlsruhe Inst. f. angewandte Kernphysik, 75 Karlsruhe, W. Germany.

[1]K. Fischer, H. Bilz, R. Haberkorn, and W. Weber, Phys. Status Solidi B **54**, 285 (1972).

[2]K. Fischer, Phys. Status Solidi B **66**, 295 (1974).

[3]B. Dorner, W. von der Osten, and W. Bührer, J. Phys. C **9**, 723 (1976).

[4]W. G. Kleppmann and H. Bilz, Commun. Phys. **1**, 105 (1976).

[5]W. G. Kleppmann, J. Phys. C $\underline{9}$, 2285 (1976).

[6]R. Zeyher, Phys. Rev. Lett. $\underline{35}$, 174 (1975).

[7]C. M. Varma and W. Weber, Phys. Rev. Lett. $\underline{39}$, 1094 (1977).

[8]C. M. Varma and W. Weber, Phys. Rev. B. $\underline{19}$, 6142 (1979).

[9]C. M. Varma, E. I. Blount, P. Vashishta, and W. Weber, Phys. Rev. B $\underline{19}$, 6130 (1979).

[10]W. Weber (unpublished).

[11]See, e.g., L. J. Sham, in *Dynamical Properties of Solids*, edited by G. K. Horton and A. A. Maradudin (North-Holland, Amsterdam, 1974).

[12]J. C. Slater and G. F. Koster, Phys. Rev. $\underline{94}$, 1498 (1954).

[13]J. S. Wang, M. Schlüter, and M. L. Cohen, Phys. Status

Solidi B $\underline{77}$, 295 (1976).

[14]P. V. Smith, J. Phys. Chem. Solids $\underline{37}$, 581 (1976); $\underline{37}$, 589 (1976).

[15]J. B. Diamond, in *Computational Methods in Band Theory*, edited by T. M. Marcus, J. S. Janak, and A. R. Williams (Plenum, New York 1971).

[16]J. A. Appelbaum and D. R. Hamann, in *Transition Metals, 1977*, edited by J. G. Lee, J. M. Perez, and E. Fawcett, IOP Conf. Ser. No. 39 (IPPS, London, 1978).

[17]F. Herman and S. Skillman, *Atomic Structure Calculations* (Prentice-Hall, Englewood Cliffs, 1963).

[18]P. R. Vijayaraghavan, R. M. Nicklow, H. G. Smith, and M. K. Wilkinson, Phys. Rev. B $\underline{1}$, 4819 (1970).